Pflugers Arch - Eur J Physiol (2006) 453:53–66
DOI 10.1007/s00424-006-0110-5

CELL AND MOLECULAR PHYSIOLOGY

Impact of post-synaptic block of neuromuscular transmission, muscle unloading and mechanical ventilation on skeletal muscle protein and mRNA expression

H. Norman · J. Nordquist · P. Andersson · T. Ansved · X. Tang · B. Dworkin · L. Larsson

Received: 7 April 2006 / Revised: 11 May 2006 / Accepted: 30 May 2006 / Published online: 26 July 2006

Abstract To analyse mechanisms of muscle wasting in intensive care unit patients, we developed an experimental model where rats were pharmacologically paralysed by post-synaptic block of neuromuscular transmission (NMB) and mechanically ventilated for 9±2 days. Specific interest was focused on the effects on protein and mRNA expression of sarcomeric proteins, i.e., myosin heavy chain (MyHC), actin, myosin-binding protein C (MyBP-C) and myosin-binding protein H (MyBP-H) in fast- and slow-twitch limb, respiratory and masticatory muscles. Muscle-specific differences were observed in response to NMB at both the protein and mRNA levels. At the protein level, a decreased MyHC-to-actin ratio was observed in all muscles excluding the diaphragm, whereas at the mRNA level a decreased expression of the dominating MyHC isoform(s) was observed in the hind limb and intercostal muscles, but not in the diaphragm and masseter muscles. MyBP-C mRNA expression was decreased in the limb muscles, but it otherwise remained unaffected. MyBP-H conversely increased in all muscles. Furthermore, we found myofibrillar protein and mRNA expression to be affected differently when comparing NMB animals with peripherally denervated (DEN) ambulatory rats. We report that NMB has both a larger and different impact on muscle, at the protein and mRNA levels, than DEN has.

Keywords Myosin · Actin · Neuromuscular blockade · Immobilisation · Mechanical ventilation

H. Norman · J. Nordquist · P. Andersson · L. Larsson (✉)
Department of Neuroscience/Clinical Neurophysiology,
Uppsala University,
SE-751 85 Uppsala, Sweden
e-mail: Lars.Larsson@neurofys.uu.se

T. Ansved
Karolinska Institute,
Stockholm, Sweden

X. Tang · B. Dworkin
Hershey Medical Centre,
Pennsylvania State University College of Medicine,
Hershey, PA, USA

L. Larsson
Centre for Development and Health Genetics,
Pennsylvania State University,
University Park, PA, USA

Introduction

Over the past decades, the treatment of critically ill intensive care unit (ICU) patients has improved dramatically, resulting in a significantly better survival rate. However, a follow-up study on critical illness survivors reported persistent muscle weakness and fatigue in all survivors [17], naming neuromuscular abnormalities as the dominant cause of the reduced health-related quality of life in critically ill ICU survivors. Because the pathophysiology of post-ICU disability remains unknown, there is a need for research on the mechanisms underlying muscle wasting and the consequent motor handicap [24].

Several different rodent models such as peripheral denervation [5, 32], immobilisation by casting [3, 11] and unloading by hind limb by suspension [4, 11, 48] have been used to study muscle wasting. Although these methods all successfully induce muscle atrophy, they each do so via different effects on muscle structure and function and have different underlying cellular mechanisms. These differences are especially consequential, given evidence that the muscle wasting in ICU patients is anatomically specific. For example, the severe muscle wasting and muscle paralysis

associated with a preferential loss of the motor protein myosin, as in acute quadriplegic myopathy (AQM), affect primarily spinal nerve innervated muscles, while cranial nerve innervated muscles are spared or less affected [29]. This loss of myosin is associated with a down-regulation of protein synthesis at the transcriptional level and enhanced myofibrillar protein degradation [7, 8, 16, 39, 46]. Because the traditional atrophy models do not realistically approximate the actual treatment environment of ICU patients, i.e., mechanical ventilation and immobilisation by post-synaptic pharmacological blockade, they may not adequately emulate the clinical syndrome. An experimental animal preparation that accurately models the clinical state of ICU patients would provide a vehicle for the analysis of mechanisms and pre-clinical evaluation of therapeutic interventions. We propose that the experimental animal model developed by Dworkin et al. [10] is such a preparation, which mimics the muscle unloading in ICU patients by long-term post-synaptic pharmacological block of neuromuscular transmission and mechanical ventilation.

We will show evidence for dramatic muscle-specific changes in myofibrillar mRNA and protein expression in response to prolonged post-synaptic block of neuromuscular transmission block. Furthermore, quantitative and qualitative differences in myofibrillar mRNA and protein expression were observed between the rat ICU and peripheral denervation models of muscle wasting (1 to 2 weeks of NMB, muscle unloading and mechanical ventilation, were typically more pronounced than 3 weeks of peripheral denervation).

Materials and methods

Animals

Thirteen (306±34 g) female Sprague–Dawley rats were included in this study, i.e., five animals in the experimental group and eight in the control group. The experimental rats were anesthetised, pharmacologically paralysed and mechanically ventilated for 7–13 (9±2) days. The experiments were terminated due to failure of electrodes, which resulted in variable experimental durations, and the animals were euthanised while sedated. In no case did animals show any signs of infections or septicaemia. In a previous study, we analysed the effects of 21 days of peripheral unilateral denervation on the morphological properties of skeletal muscle in young, adult and old male Wistar rats [2]. In that study, unilaterally denervated soleus and extensor digitorum longus (EDL) muscles were analysed 3 weeks after denervation, together with contralateral control muscles from six young (5 months, 414±21 g) animals. The muscle tissue from the denervation study was included and all muscles from neuromuscular blocked (NMB) and denervated (DEN) rats have been analysed in an identical way. The Institutional Animal Care and Use Committee at the Pennsylvania State University College of Medicine and the Ethical Committee at the Karolinska Institute approved all aspects of this study.

The mechanically ventilated, with the central nervous system intact, NMB rats were individually and carefully maintained with the use of monitoring, life support and analgesic protocols as stringent as those that are accepted for the critical care of human adults and infants [10]. All actual surgery or physical manipulation were done under precisely controlled and carefully monitored deep (>1.5%) isoflurane anaesthesia, and adequate amounts of amino acids were given to maintain a positive nitrogen balance. The NMB rats were studied one at a time and attended round the clock. To induce neuromuscular blockade, the animals were treated with an initial intra-arterial injection of 100 μg α-cobratoxin, followed by continuous infusion at 60 μg/day. In addition, the experimental method and procedures developed by Dworkin et al. [10], which have been presented in detail elsewhere, were followed and an overview of the treatment of NMB animals is given in Table 1. Eight age-, gender- and strain-matched animals were used as controls. The rats were euthanised with a 1-ml intravenous air bolus, and the soleus, EDL, tibialis anterior (TA), intercostal (frontal half from the tenth intercostal space), frontal half of the diaphragm and the superficial part of the masseter muscles were dissected bilaterally. The same muscles were collected from controls.

In a previous study, the sciatic nerve was cut unilaterally in the proximal part of the hind limb, approximately a 15- to 20-mm-long section of the nerve was removed and the soleus and EDL were collected on both the DEN and contralateral (DEN control) sides 3 weeks after denervation [2].

All muscles in NMB, control, DEN and DEN control rats were collected immediately after euthanasia, quickly frozen in Freon, isopentane or propane cooled by liquid nitrogen and stored at −80°C for further analyses. The analyses of all muscle tissues took place simultaneously. The soleus, EDL and TA muscles were weighed upon dissection.

Enzyme histochemistry

The frozen samples were cut at their greatest girth perpendicular to the longitudinal axis of muscle fibres into 10-μm-thick cross-sections with a cryotome (2800 Frigocut E, Reichert-Jung, Heildelberg, Germany) at −20°C. The muscle fibres in the cross-sections were stained for myofibrillar ATPase after alkaline (2.253 g glycine, 2.4 g $CaCl_2$, 1.755 g NaCl and 300 ml distilled H_2O) and acid preincubations (3.90 g Na–acetate, 3.7 g KCl and 500 ml distilled H_2O), NADH (3.2 mg NADH, 8.0 mg NBT, 2.0 ml

Table 1 Neuromuscular blocked animals

Animal	Duration of mechanical ventilation (days)	Pre-Experiment Body weight (g)	Post-Experiment Body weight (g)	NMB	CS	Antibiotics	Nutrition
1	7	329	–	α-Cobratoxin (60 μg/day)	Hydrocortisone sulfate (16 mg/kg)	Tobramycin sulfate (4.5 mg/kg); oxacillin sodium (150 mg/kg); ticarcillin disodium	Ringers, H_2O, glucose, K+, canrenoate
2	8	394	303	α-Cobratoxin (60 μg/day)	Hydrocortisone sulfate (16 mg/kg); 10 mg intravenously administered over days 5–8	Tobramycin sulfate (4.5 mg/kg); oxacillin sodium (150 mg/kg); ticarcillin disodium	Ringers, H_2O, glucose, K+, canrenoate
3	13	294	180	α-Cobratoxin (60 μg/day)	Hydrocortisone sulfate (16 mg/kg); 10 mg intravenously administered over days 5–8	Tobramycin sulfate (4.5 mg/kg); oxacillin sodium (150 mg/kg); ticarcillin disodium	Ringers, H_2O, glucose, K+, canrenoate
4	9	263	190	α-Cobratoxin (60 μg/day)	Hydrocortisone sulfate (16 mg/kg)	Tobramycin sulfate (4.5 mg/kg); oxacillin sodium (150 mg/kg)	Ringers, H_2O, glucose, K+, canrenoate
5	9	278	200	α-Cobratoxin (60 μg/day)	Hydrocortisone sulfate (16 mg/kg)	Tobramycin sulfate (4.5 mg/kg); oxacillin sodium (150 mg/kg)	Ringers, H_2O, glucose, K+, canrenoate

Duration of mechanical ventilation, pharmacology and nutrition of NMB animals, including pre- and post-experiment body weight
CS Corticosteroids, *NMB* neuromuscular blocking agents

MOPS solution and 8.0 ml distilled H_2O) and haematoxylin and eosin. The fibres were classified according to the pH sensitivity of the myofibrillar ATPase, type I ATPase fibres being those with acid stable ATPase (after pre-incubation at pH 4.3) and with alkali-labile ATPase (after pre-incubation at pH 10.3) and type II ATPase fibres being those showing the reverse pH sensitivity. Type II ATPase fibres were further subdivided into types IIA and IIB ATPase fibres, the former being inhibited at pH 4.5. Type IIA fibres express MyHCIIa and type IIB fibres express MyHCIIb, MyHCIIx or a combination of MyHCIIx and MyHCIIb [28]. The cross-sectional area of each muscle fibre type was measured semi-automatically on the mATPase stained section (pH 4.5) with the aid of a digitising unit connected to a microcomputer (Videoplan, Kontron Bildanalyse, Munich, Germany).

Myofibrillar protein separations

For measuring the relative contents of myosin heavy chain (MyHC) and actin in muscle specimens and for calculating the myosin isoform composition, two 10-μm cross-sections of each muscle were dissolved in urea buffer (120 g urea, 38 g thiourea, 70 ml H_2O, 25 g mixed bed resin, 2.89 g dithiothreitol, 1.51 g Trizma base, 7.5 g sodium dodecyl sulfate (SDS) and 0.004% bromophenol blue) and a volume of 4 μl was loaded on 6 and 12% sodium dodecyl sulfate-polyacrylamide gel electrophoresis (SDS-PAGE). The total acrylamide and Bis concentrations were 4% in the stacking gel and 6 and 12% in the running gel, for the respective gels. The gel matrix included 30 and 10% glycerol in the 6 and 12% SDS-PAGE, respectively, as described previously [30]. In brief, electrophoresis was performed at a constant current of 16 mA for 5 h with a Tris–glycine electrode buffer (pH 8.3) at 15°C (SE 600 vertical slab gel unit, Hoefer Scientific Instruments, San Francisco, CA, USA).

The 12% gels were stained with Coomassie blue (0.5 g brilliant blue, 225 ml MeOH, 225 ml distilled H_2O and 50 ml acetic acid), as this staining shows high reproducibility and the ability to penetrate the gel and stain all proteins present, i.e., allowing accurate quantitative protein analyses. Separating gels for 6% SDS-PAGE were silver-stained, due to high sensitivity [13]. All gels were subsequently scanned in a soft laser densitometer (Molecular Dynamics, Sunnyvale, CA, USA) with a high spatial resolution (50 μm pixel spacing) and 4,096 optical density levels to determine the relative contents of MyHC isoforms. The volume integration function was used to quantify the amount of protein on 12 and 6% gels (ImageQuant TL Software v. 2003.01, Amersham Biosciences, Uppsala, Sweden).

Western blot

The samples were dissolved in urea buffer (120 g urea, 38 g thiourea, 70 ml H_2O, 25 g mixed bed resin, 2.89 g dithiothreitol, 1.51 g Trizma base, 7.5 g SDS and 0.004% bromophenol blue) and loaded onto a 12% SDS-PAGE (see above). The proteins were transferred overnight at 250 mA using a nitrocellulose membrane immersed in transfer buffer (144 g glycine, 30 g tris base and 1 g SDS). The membrane was stained with BLOT-fast stain (Geno Technology, St. Louis, MO, USA) to ensure a good transfer, and the remaining gel was stained to determine if a sufficient amount of protein was transferred.

For detection of MyHC degradation, an immunoblot was run using the membrane from the Western blot. Immunoblotting involved, first, blocking the membrane with saturation buffer [4.44 g 50 mM Tris–HCl, pH 8.0 (25°C), 2.65 g Trizma base, 0.294 g 2 mM $CaCl_2$, 4.967 g 85 mM NaCl and 5% non-fat dry milk], followed by incubations with the primary antibody (Rabbit anti-myosin 18-0074, Zymed Laboratories, San Francisco, CA, USA) and the secondary antibody (Biotinylated anti-rabbit IgG BA-1000, Vector Laboratories, Burlingame, CA, USA), with intermittent washing steps using the wash buffer [4.44 g 50 mM Tris–HCl, pH 8.0 (25°C), 2.65 g Trizma base, 0.294 g 2 mM $CaCl_2$, 4.967 g 85 mM NaCl, 0.1% non-fat dry milk and 0.1% Tween 20]. The membrane was then incubated in alkaline-phosphatase streptavidin buffer [6.35 g 50 mM Tris–HCl, pH 7.5 (25°C), 1.18 g Trizma base, 8.76 g 150 mM NaCl and 0.1% Tween 20] and subsequently developed using colour development buffer (NBT/BCIP, 12.11 g 100 mM Tris, pH 9.5). The membrane was scanned using a soft laser densitometer (Molecular Dynamics, Sunnyvale, CA, USA).

RNA purification

The RNA for quantitative real-time polymerase chain reaction (RT-PCR) was extracted from frozen muscle tissue (10–30 mg) using a Qiagen RNeasy® Mini Kit (Qiagen, Valencia, CA, USA). Muscle tissue was homogenised using a rotor homogeniser (Eurostar Digital, IKA-Werke). QIAshredder™ columns (Qiagen, Valencia, CA, USA) were used to disrupt DNA. Total RNA was eluted from RNeasy® Mini columns with 30 μl of RNase-free water. The RNA concentrations were then quantified using the fluorescent nucleic acid stain, Ribogreen® (Molecular Probes, Eugene, OR, USA), on a Hitachi F-4000 fluorescence spectrophotometer.

cDNA preparation

cDNA was prepared using Ready-To-Go™ You-Prime First-Strand-Beads (Amersham Biosciences, Uppsala, Sweden) according to the instructions from the manufacturer. Total RNA (100 ng) was used to synthesise cDNA, using 0.66 μg random hexamers (Amersham Biosciences, Uppsala, Sweden) and 0.5 μg oligo-dT primers (Amersham Biosciences, Uppsala, Sweden). The cDNA was diluted to a volume of 100 μl and stored at −80°C until quantification by real-time PCR.

Quantitative real-time PCR

Real-time PCR was used to quantify the mRNA levels for rat MyHCs (types I, IIa, IIx and IIb), skeletal α-actin, myosin-binding protein C (MyBP-C) and myosin-binding protein H (MyBP-H) (GenBank accession numbers X15939, L13606, AF157005, L24897, NM_019212, X90475 and BC061993, respectively). Taqman primers and probes were designed using the software Primer Express® (Applied Biosystems, Foster City, CA, USA). The sequences for primers and probes are listed in Table 2. The probes, labelled with FAM (*N*-(3-fluoranthyl)maleimide), and primers were purchased from Thermo Electron (Thermo Electron, Ulm, Germany). All primers and probes were purified by high-performance liquid chromatography. SYBR Green (1988123, Roche Diagnostics, Germany) was used for detection of MyBP-H and MyBP-C, as well as for 18S when it was used as an internal standard for MyBP-H and MyBP-C.

Real-time PCR was run using the sequence detection system, ABI PRISM® 7700 (Applied Biosystems, Foster City, CA, USA). The AmpliTaq Gold DNA polymerase was heat-activated at 95°C for 10 min, followed by 40 cycles of a two-step PCR with denaturation at 95°C for 15 sec and a combined annealing and extension step at 60°C for 1 min. The PCR was performed in a volume of 25 μl, which included 0.4 μM of each primer and 0.2 μM of probe. When optimising each PCR, the PCR products were run on 2% agarose gels to ensure that primer-dimer formation was not occurring. Only one product of expected size was detected in all cases. Each sample was run in triplicates. With each PCR run, a standard cDNA was included in triplicates of three concentrations comprising a standard curve. A control sample was used for the standard. Finally, the negative controls without cDNA were included on each plate.

Analysis of RT-PCR data

Sequence detection software 1.6.3 (Applied Biosystems, Foster City, CA, USA) was used to analyse the raw real-time PCR data. The threshold cycle (C_T) data acquired from the real-time PCR run was related to the standard curve to obtain the starting quantity (SQ) of the template cDNA for each sample. Each sample in a triplicate had to be within 0.5 C_T of each other to be included in the analysis. The triplicates of each sample were averaged and the SQ of the

Table 2 RT-PCR primers and probes

Gene	Forward primer	Probe	Reverse primer	Product length
MyHCIIa	GGCCAGAGTGCGTGAACTG	AGGGTGAGGTAGAGAGTGAG CAGAAGCGG	AAGCCCTTTGACAGCCTCAA	73
MyHCIIb	GAGCTTGAAAACGAGG TGGAAA	TGAACAGAAGCGCAACATT GAAGCT	TGCTTGCGAAGACCCTTGA	68
MyHCIIx	TCGCCGAGTCCCAGGTC	ACAAGCTGCGGGTGAAG AGCCG	CGCTTATGATTTTGGTGTGAACC	66
MyHCTypeI	CTGCGATGCAACGGAGTG	AGGGTATCCGCATCTGTAGG AAGGGCTT	GCCGGAAGTCCCCATAAAGA	82
α-Actin	AGGTCATCACCATCGGCAAT	AGCGCTTCCGTTGCCCGGA	AAGGAAGGCTGGAAGAGCGT	61
MyBP-C	GGCGTGCCTCCAAACATAAT	SYBR Green	ATTCCTCCGGATTGCTTGACT	64
MyBP-H	ACCTCATCATTGGCAACTCGTA	SYBR Green	CACTGAGGCCACACAGGTTTT	63
18S	GTGCATGGCCGTTCTTAGTTG	TGGAGCGATTTGTCTGGTTAA TTCCGATAAC or SYBR Green	AGCATGCCGAGAGTCTCGTT	74

sample was related to the triplicate average of the internal standard, 18S (GenBank accession number AF102857). The sequences for 18S primers and probes are listed in Table 2. The ribosomal RNA 18S was chosen as an internal standard, as it was not affected by the experiment. The standard curves for both the gene of interest and 18S were included on each plate. To be accepted, the slopes of the standard curves had to be between −3.0 and −3.5 and were not allowed to differ by more than 5%. The values of the samples, related to the standard, were then analysed.

As the development of primers and probes, for use in real-time PCR, for all MyHC isoforms was not possible, an alternative calculation was used to determine total MyHC mRNA. The percentage of myosin isoform, as determined from 6% SDS-PAGE (Table 4), which was silver-stained and scanned using a soft laser densitometer (see above), was related to its corresponding mRNA expression. For example, if the MyHCIIa isoform comprised 33% of the total MyHC protein, as determined by 6% SDS-PAGE, the mRNA starting quantity value for MyHCIIa was calculated to comprise 33% of total MyHC mRNA. The total MyHC mRNA was also used when calculating the MyHC-to-actin mRNA ratios. This method was decided upon based on reports that the mRNA signals in skeletal muscles change in parallel, in relative intensity, with the MyHC protein expression pattern [15, 31, 49].

Statistics

The mean and standard deviation (SD) of means were calculated by standard procedures. When comparing two groups (i.e., NMB vs control, diaphragm and masseter analysis), an unpaired Student's *t* test was used when appropriate. When the normality test failed, the non-parametric Mann–Whitney rank sum test was used. One-way analysis of variance (ANOVA) was used to compare all four groups (i.e., NMB, control, DEN and DEN contralateral control). When the normality test failed, a one-way ANOVA on ranks, i.e., Kruskal–Wallis one-way ANOVA, was used. Two-way ANOVA was performed to compare the interaction between the type of treatment, i.e., NMB vs DEN, and type of muscle, i.e., EDL vs soleus. A Tukey's post hoc contrast was performed to determine the means that were different at the significance level of $p<0.05$; when normality failed, Dunn's post hoc was used. The values were excluded if they varied more than two standard deviations from the mean. The differences were considered significant at $p<0.05$.

Results

Muscle mass and muscle fibre size

There was no difference in body weight between control and pre-experiment NMB rats. Nine (9±2) days of blocked neuromuscular transmission and muscle unloading resulted in a 28% decrease in body weight ($p<0.001$, 210±50 vs 290±40 g). The decreased body weight was paralleled by a 41, 25 and 35% decrease in muscle weights in the soleus ($p<0.001$, 79±17 vs 122±18 mg), EDL ($p<0.01$, 97±21 vs 127±19 mg) and TA ($p<0.01$, 369±66 vs 569±22 mg), respectively. The decreased muscle weight was accompanied by a decrease in muscle fibre size. In the slow-twitch soleus, type I and IIA muscle fibre size was 44 and 46% smaller ($p<0.001$) than in controls. In the EDL, the average cross-sectional area of type I, IIA and IIB fibres were 37, 22 and 36% smaller than in the controls, respectively, but statistically significant differences were restricted to type IIB ($p<0.01$) and type I ($p<0.01$) fibres (Fig. 1; Table 3).

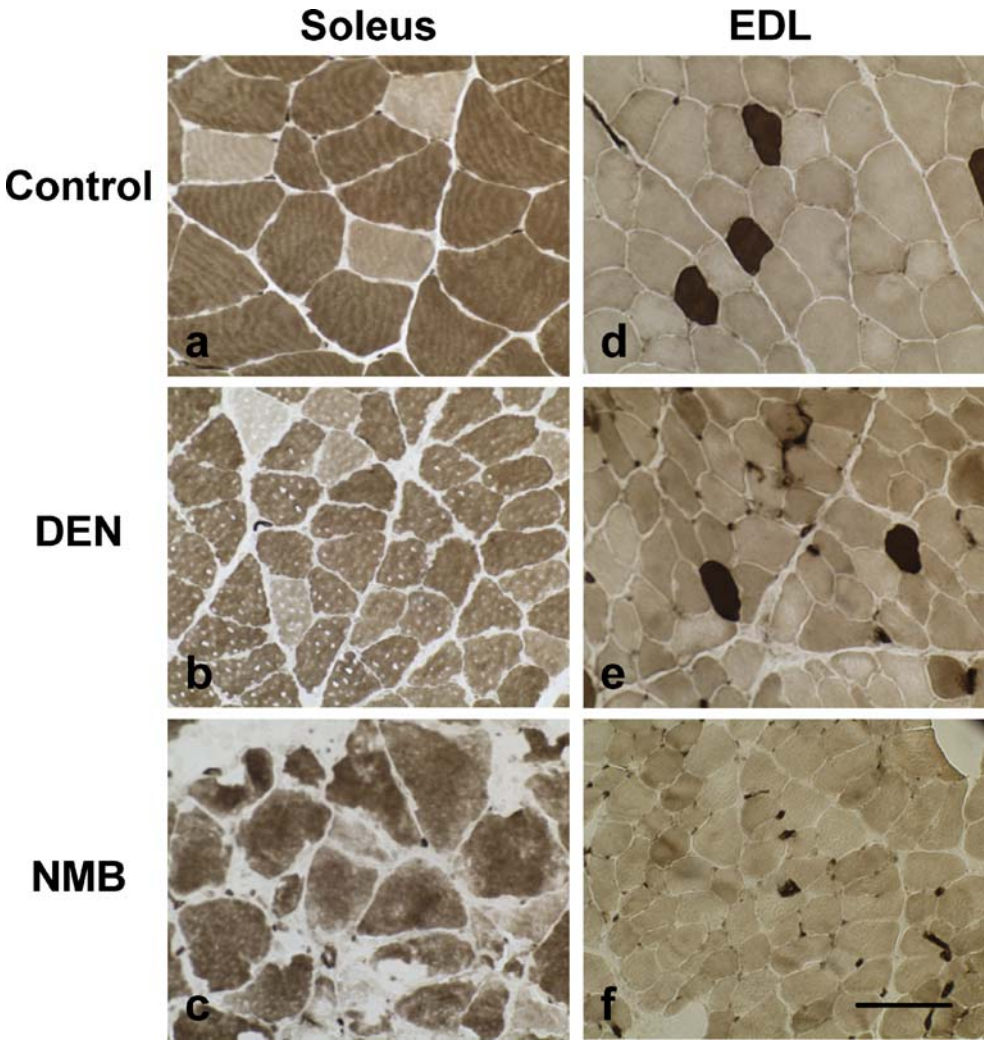

Fig. 1 Enzyme histochemistry of muscle biopsy cross-sections. Enzyme histochemical myofibrillar ATPase, pH 4.5, staining of control, DEN and NMB soleus (**a**–**c**) and EDL (**d**–**f**) muscles, respectively. *Bar*, 200 μm

The lack of a statistically significant difference in the type IIA fibres is, at least in part, due to the smaller number of this fibre type. A methodological error related to a non-perpendicular cut of the muscle appears less likely as significant differences in the smaller diameter of type I (p<0.001, 22±1 vs 28±2 μm) and type IIB (p<0.01, 28±3 vs 36±4 μm) fibres were observed between NMB rats and controls, while the smaller type IIA fibre diameter appeared to decrease but failed to reach the level of statistical significance (p=n.s., 31±4 vs 37±8 μm).

Table 3 Cross-sectional area (μm^2) of type I and type II fibres measured on mATPase stained sections after acid preincubation (pH 4.5)

Muscle section	Animal	I	IIA	IIB
EDL	Control	860±80	1,480±650	1,410±300
	NMB	570±30**	1,130±280	870±160**
Soleus	Control	2,420±360	1,620±200	–
	NMB	1,360±180***	880±160***	–

**p<0.01; ***p<0.001 (significance vs control group)

Myofibrillar protein and mRNA expression

In NMB rats, myosin–actin protein ratios were significantly lower in the EDL (p<0.001), soleus (p<0.001), intercostal (p<0.001) and masseter muscles (p<0.01) than in controls, but there was no significant difference in the diaphragm (Fig. 2a). Immunoblots did not detect any consistent proteolytic myosin bands in any of the hind limb, respiratory or masticatory muscles after 9 days NMB or in control animals (data not shown).

In the fast-twitch EDL, MyHC protein isoform expression differed significantly between NMB animals and controls, i.e., a 27% higher (p<0.05) proportion of MyHCIIa was observed in the NMB rats indicating a type MyHCIIb→MyHCIIx→MyHCIIa isoform transition in

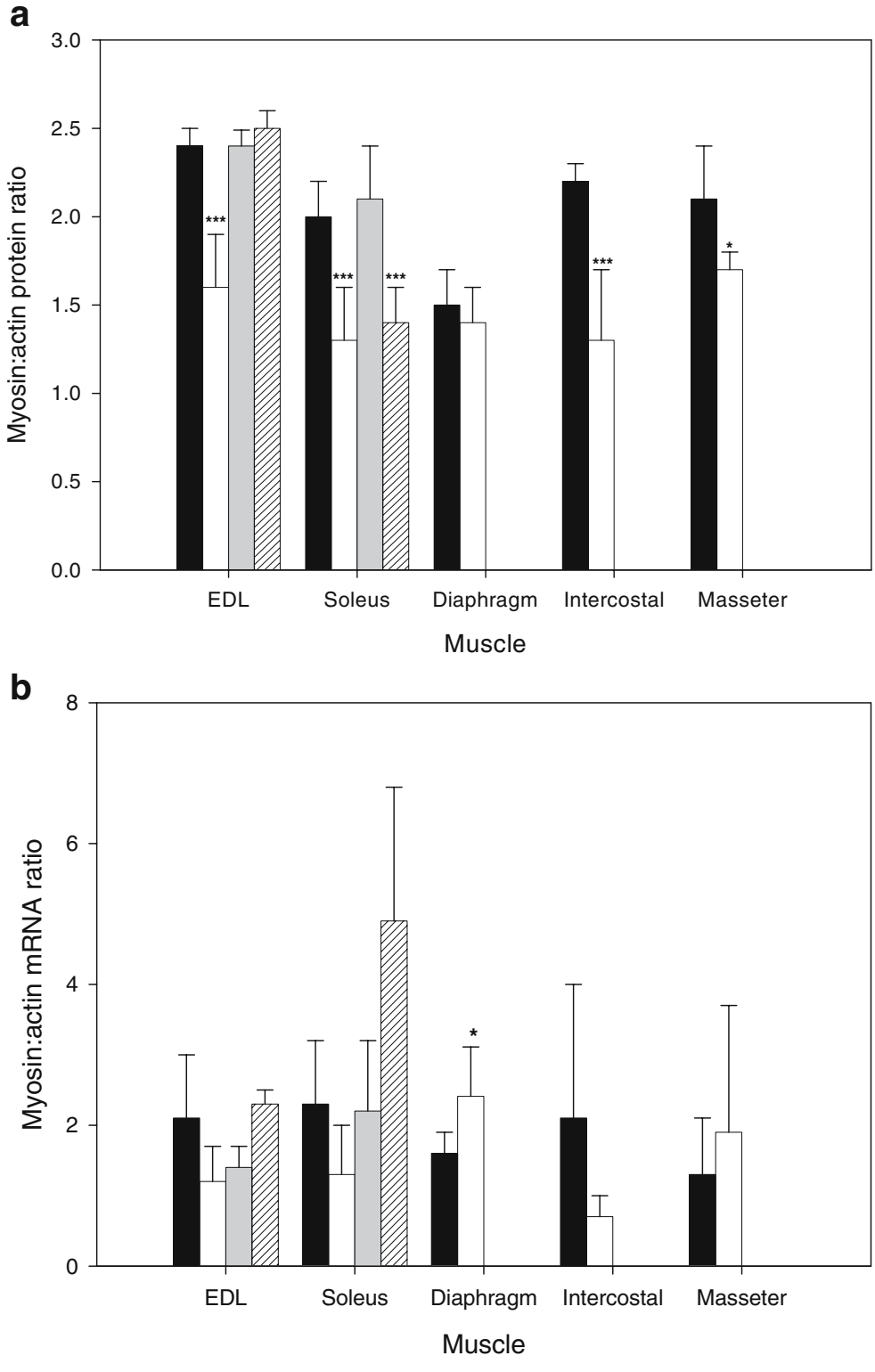

Fig. 2 Myosin–actin ratios. Myosin–actin ratios for the EDL, soleus, diaphragm, intercostal and masseter muscles for **a** protein levels, as determined by 12% SDS-PAGE, and **b** mRNA levels, as determined by real-time PCR, of control (*filled bar*), NMB (*open bar*), DEN control (*grey bar*) and DEN (*hashed bar*). *$p<0.05$; ***$p<0.001$ (statistically significant differences between experimental groups and controls)

response to NMB and unloading (Table 4). This is supported by the lower ($p<0.01$–0.001) MyHCIIx and MyHCIIb mRNA levels in NMB than in control animals (Table 5). In the slow-twitch soleus, there was no significant change in MyHC isoform protein expression between NMB and controls. However, MyHCI mRNA expression was lower ($p<0.001$) and a trend ($p<0.1$) towards decreased mRNA expression was seen for MyHCIIa (Table 5). Thus, a significant decrease in myosin mRNA expression was observed in the myosin isoforms dominating both the fast-

Table 4 Myosin isoform composition as determined by 6% SDS-PAGE for neuromuscular blocked and control animals in the extensor digitorum longus, soleus, intercostal, diaphragm and masseter muscles

Muscle section	Animal	I	IIa	IIx	IIb
EDL	NMB	<1	27±8*	45±13	32±9
	Control	<1	0	57±12	43±13
Soleus	NMB	86±12	13±11	–	–
	Control	93±5	7±5	–	–
Intercostal	NMB	3±0	8±4	50±11	39±19
	Control	4±3	15±9	56±13	26±14
Diaphragm	NMB	25±12	34±5	42±10	–
	Control	27±4	32±3	41±7	–
Masseter	NMB	–	–	54±30	46±30
	Control	–	–	59±41	51±39

Values are percentage±standard deviation
*$p<0.05$ (significance of NMB vs control group)

twitch EDL and the slow-twitch soleus in response to 9 days NMB and unloading.

In respiratory and masticatory muscles, MyHC protein isoform expression did not differ between NMB animals and controls (Table 4). At the mRNA level, the three muscles were affected differently by the intervention. In the intercostal muscles, a significant decline ($p<0.05$–0.001) was observed for all MyHC isoforms (Table 5). In the other respiratory muscle, the diaphragm, a lower ($p<0.01$) MyHCI mRNA expression was observed in the NMB animals than in controls, but only a trend ($p<0.1$) towards a lower mRNA level was observed for the dominating MyHCIIx isoform, while no change for the MyHCIIa isoform was found (Table 5). In the masseter, no significant differences were seen for either MyHCIIx or MyHCIIb, although there was a trend ($p<0.1$) toward a lower MyHCIIx mRNA expression in the NMB rats than in the controls (Table 5).

Skeletal muscle α-actin mRNA expression was lower ($p<0.05$–0.001) in NMB animals than in controls for all muscles, although the masseter and intercostal muscles appeared to be less affected than the limb muscles (Table 5). The mRNA levels of the myosin-associated protein MyBP-C was lower ($p<0.01$–0.001) in the limb muscles but not in the respiratory or masticatory muscles (Table 5). In contrast to the other myofibrillar proteins, the mRNA levels of the

Table 5 Starting quantity of mRNA values for pharmacologically neuromuscular blocked, control, denervated and DEN contralateral control rats in the extensor digitorum longus, soleus, diaphragm, intercostal and masseter muscles

Muscle section	Animal	MyHCI	MyHCIIa	MyHCIIx	MyHCIIb	α-Actin	MyBP-C
EDL	NMB	–	0.04±0.04 (n=5)	0.3±0.2*** (n=5)	0.3±0.2** (n=5)	0.3±0.1*** (n=5)	0.7±0.2** (n=5)
	Control	–	0.2±0.2 (n=8)	1.0±0.3 (n=8)	2.0±0.9 (n=8)	0.8±0.2 (n=8)	1.2±0.3 (n=8)
	DEN	–	0.02±0.03 (n=6)	0.5±0.1** (n=4)	0.7±0.3** (n=5)	0.2±0*** (n=5)	0.6±0.2*** (n=6)
	DEN Control	–	0.5±0.4 (n=6)	1.3±0.3 (n=6)	2.0±1.0 (n=6)	1.0±0.4 (n=6)	1.8±0.3 (n=6)
Soleus	NMB	0.1±0.1*** (n=5)	0.1±0.2 (n=5)	–	–	0.1±0** (n=5)	0.5±0.3** (n=5)
	Control	0.9±0.2 (n=8)	0.4±0.2 (n=8)	–	–	0.4±0.3 (n=8)	1.0±0.1 (n=8)
	DEN	0.4±0.2** (n=6)	0.1±0.1 (n=6)	–	–	0.1±0*** (n=6)	0.5±0.2*** (n=6)
	DEN Control	1.1±0.2 (n=6)	0.1±0.1 (n=6)	–	–	0.5±0.1 (n=6)	1.3±0.2 (n=6)
Diaphragm	NMB	0.2±0.2** (n=5)	0.7±0.5 (n=5)	0.8±0.4 (n=5)	–	0.3±0.1*** (n=5)	0.7±0.4 (n=5)
	Control	0.7±0.3 (n=8)	0.8±0.3 (n=8)	1.4±0.7 (n=8)	–	0.6±0.1 (n=8)	1.0±0.2 (n=7)
Intercostal	NMB	0.3±0.4*** (n=5)	0.2±0.3* (n=5)	0.2±0.1*** (n=5)	0.1±0.1** (n=5)	0.2±0.2* (n=5)	1.8±2.0 (n=5)
	Control	1.1±0.4 (n=6)	0.6±0.3 (n=6)	1.7±0.1 (n=6)	0.6±0.4 (n=6)	0.5±0.2 (n=6)	1.7±2.3 (n=6)
Masseter	NMB	–	–	0.4±0.3 (n=5)	0.4±0.3 (n=5)	0.4±0.3* (n=5)	1.8±0.5 (n=5)
	Control	–	–	1.1±0.7 (n=8)	0.5±0.3 (n=8)	0.8±0.3 (n=8)	1.4±0.5 (n=8)

If the gene was not present or comprised an insignificant amount of protein expression in the muscle, as determined by 6% SDS-PAGE, measurement was not performed. The values are SQ±standard deviation
*$p<0.05$; **$p<0.01$; ***$p<0.001$ (significance of NMB vs control group or DEN vs DEN contralateral control)

myosin-associated protein MyBP-H were dramatically increased in response to NMB. That is, a 21-, 19-, 18-, 17- and 10-fold increase (p<0.01–0.001) in MyBP-H mRNA expression was observed in the EDL, soleus, intercostal, masseter and diaphragm muscles, respectively, in NMB animals compared with that in controls (Fig. 4).

Total myosin mRNA and myosin–actin mRNA ratios

Total MyHC mRNA expression was determined by weighing the starting quantity mRNA value according to the percentage of the corresponding protein in the muscle as determined by 6% SDS-PAGE (see "Materials and methods"). Using this method, it was found that total myosin mRNA levels in the EDL and soleus were lower (p<0.01–0.001) in NMB animals compared with that in controls. Total MyHC mRNA also decreased in the diaphragm and intercostal (p<0.01–0.001) but did not decrease in the masseter muscle in the NMB animals compared with that in controls (Fig. 3).

The myosin–actin mRNA ratios (Fig. 2b) were calculated by dividing the starting quantity for total MyHC (Fig. 3) by the starting quantity for actin (Table 4). In NMB animals, there was a trend (p<0.1) towards lower myosin–actin mRNA ratios than in controls for both the EDL and soleus. In the intercostal and masseter muscles, there was no significant difference in the myosin–actin mRNA ratio between NMB and control animals. In the diaphragm, on the other hand, the myosin–actin mRNA ratio was higher (p<0.05) in NMB animals than in controls (Fig. 2b), possibly accounting for the lack of a decreased myosin–actin protein ratio (Fig. 2a).

Effects of NMB vs peripheral denervation on limb muscle myofibrillar protein and mRNA expression

Apart from a slight difference in EDL MyHCIIa mRNA expression (p<0.05, 0.2±0.2 vs 0.5±0.4), there was no significant difference in MyHC mRNA and protein expression between NMB control and DEN contralateral control soleus and EDL; thus, it was assumed that a comparison between the two treatments would be adequate. In the DEN animals, a decrease (p<0.001) in MyHC-to-actin protein ratio was observed in the soleus but not in the EDL (Fig. 2a), in accordance with previous observations demonstrating a muscle-type-specific effect of peripheral denervation on the myosin–actin ratio [25]. In the NMB animals, on the other hand, the decrease in myosin–actin ratio was not restricted to a specific muscle type and a significant decrease was observed in both the fast-twitch EDL and the slow-twitch soleus. There were no signs of myosin degradation on immunoblots after either 9 days NMB or 21 days DEN in the EDL and soleus muscles (data not shown).

At the mRNA level, the expression of the MyHC isoforms dominating in the respective muscles was lower in both NMB and DEN animals than in controls, although the changes appeared to be more pronounced in NMB than in DEN rats (Table 5). For example, the MyHCIIb mRNA expression was twofold lower (p<0.05) in the EDL muscles

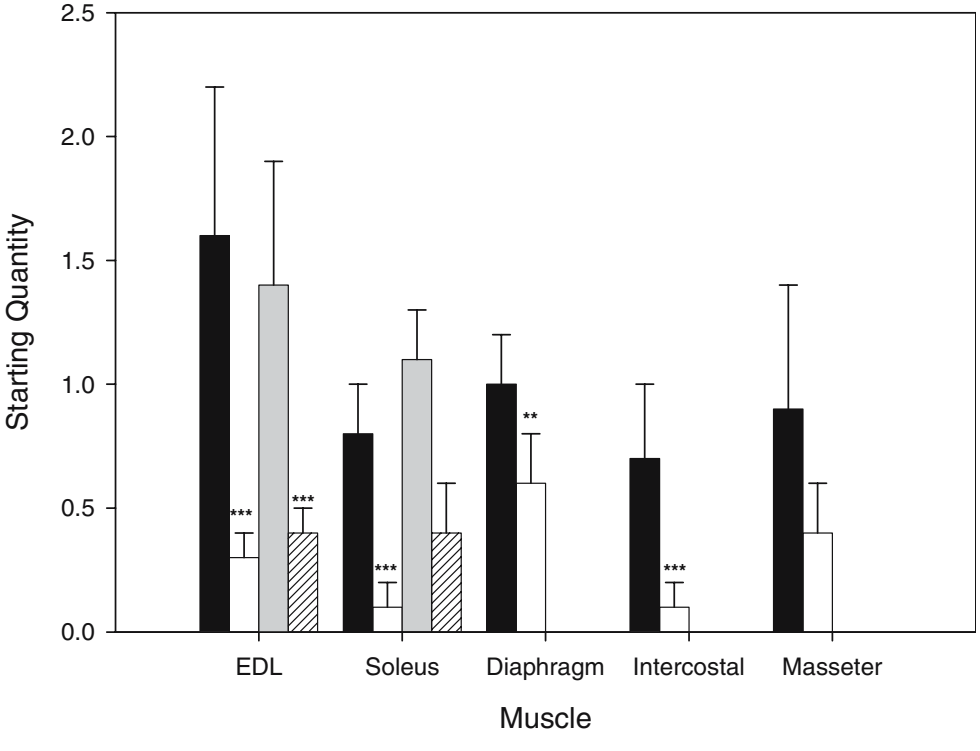

Fig. 3 Myosin mRNA expression. Expression of myosin heavy chain mRNA in the EDL, soleus, diaphragm, intercostal and masseter muscles of control (*filled bar*), NMB (*open bar*), DEN control (*grey bar*) and DEN (*hashed bar*). Myosin isoform data have been pooled for a relative starting quantity according to the "Materials and methods" section. **p<0.01; ***p<0.001 (statistically significant differences vs controls)

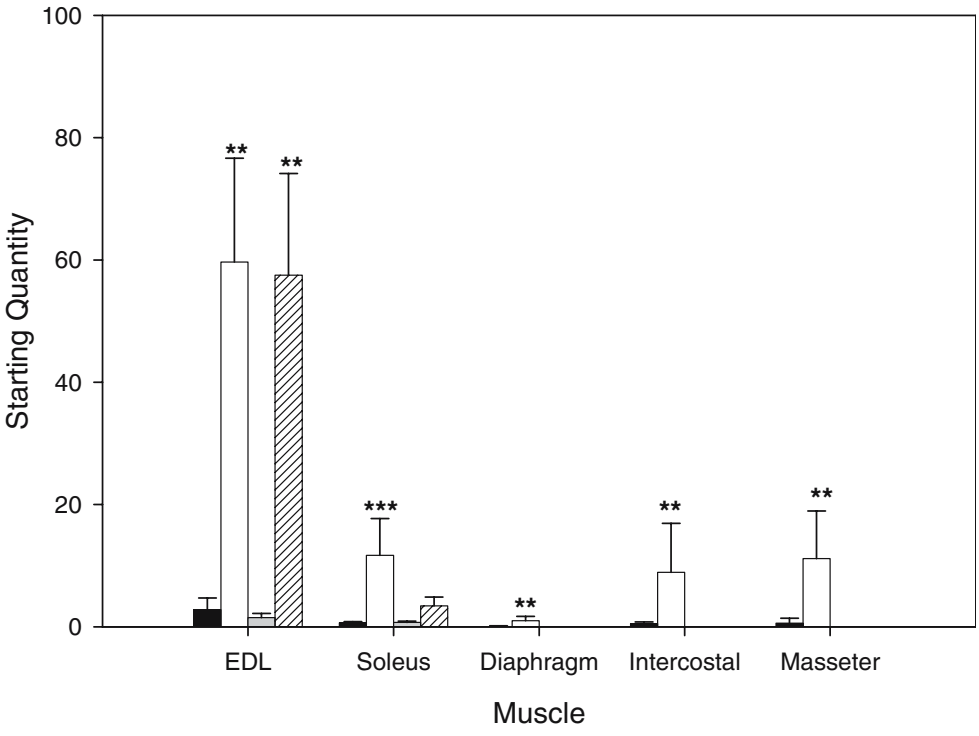

Fig. 4 MyBP-H mRNA expression. Myosin-binding protein H mRNA expression of the EDL, soleus, diaphragm, intercostal and masseter muscles in control (*black filled bar*), NMB (*open bar*), DEN contralateral control (*grey filled bar*) and DEN (*hashed bar*) rats. The values represented are the starting quantity with standard deviation. **$p<0.01$; ***$p<0.001$ (statistically significant differences vs controls)

from NMB than from DEN animals and the MyHCI mRNA levels were fourfold lower ($p<0.001$) in the soleus. In the NMB animals, the decreased MyHC-to-actin ratios in the EDL and soleus at the protein levels were paralleled by a similar decline ($p<0.05$) at the mRNA level (Fig. 2), suggesting that transcriptional regulation plays an important role in the altered expression of thick and thin filament proteins in response to NMB, unloading and mechanical ventilation. On the other hand, in the DEN animals, the changes in MyHC-to-actin protein and mRNA ratios were dissociated in the slow-twitch soleus. That is, the lower protein ratio in the soleus was accompanied by an increased mRNA ratio, resulting in a difference ($p<0.001$) in the MyHC-to-actin mRNA ratio between NMB and DEN animals (Fig. 2). Furthermore, significant interaction effects ($p<0.05$) were observed between treatment (NMB vs DEN) and muscle type in the two-way ANOVA. The outcome of the type of treatment was dissimilar ($p<0.05$–0.001) for both the EDL and soleus muscles for mRNA MyHC-to-actin ratios and significantly different ($p<0.001$) in the EDL for protein MyHC-to-actin ratios (Fig. 2). Thus, the response of skeletal muscle to peripheral denervation and NMB is different. In addition, the muscles were differentially affected by the treatments. For example, peripheral denervation affected the MyHC-to-actin ratio in the soleus and EDL differently at both the protein ($p<0.001$) and mRNA level ($p<0.01$). NMB, on the other hand, affected the soleus and EDL protein and mRNA MyHC-to-actin ratios similarly, that is, they decreased to a comparable extent (Fig. 2), suggesting that similar mechanisms are responsible for the decreased MyHC-to-actin ratio in fast- and slow-twitch muscles. In contrast, actin and the two myosin-associated proteins (MyBP-C and MyBP-H) changed in a similar pattern both at the protein and mRNA levels in NMB and DEN animals (Table 5; Fig. 4).

Discussion

To improve the quality of life in ICU survivors, it is important to have a detailed understanding of the mechanisms underlying the impaired neuromuscular function which results in muscle wasting. However, studying the mechanisms of severe muscle atrophy in patients is complicated by a number of uncontrollable factors, such as primary disease, polypharmacy and age. Therefore, the use of an animal model that mimics the ICU patient, i.e., weeks–months of immobilisation, mechanical ventilation and pharmacological paralysis (post-synaptic), facilitates the analysis of the underlying mechanisms of muscle wasting.

Rodent muscle wasting models

Several experimental animal models to induce muscle wasting have been presented to date (see [50]); however, the most commonly used models for muscle wasting lack several of the key conditions that occur in an ICU. In this study, the effects of 9 days mechanical ventilation, NMB and muscle unloading have been compared with the effects of long-term peripheral denervation on fast- and slow-

twitch hind limb muscles. In the peripheral denervation model, denervated muscles become mechanically loaded due to posture and locomotion. Emerging data shows that this mechanical loading affects gene expression. For example, the sarcomeric proteins titin and the Z-disc protein telethonin [26] are directly influenced by mechanical loading and affect gene expression.

Furthermore, the loss of an intact nerve disrupts the synaptic vesicle release from the terminal axon, but the "trophic" influence of spontaneous vesicle release is still intact in ICU patients receiving post-synaptic block of neuromuscular transmission. This has been suggested as a key difference between the effects on muscle tissue in the ICU patients and rodent models where denervation or tetrodotoxin treatments are used to induce muscle inactivity [40]. In the experimental model used in this study, limb muscles are unloaded, alpha-motoneurones are intact and the vesicle release from the terminal axon is maintained [9]. The reliable differences in myofibrillar protein and mRNA responses observed between the NMB and DEN animals may accordingly be related to differences in trophic motoneuron–muscle interactions, mechanical loading or both.

Peripheral denervation of rat hind limb muscles and chronic glucocorticoid treatment is the prevailing experimental model used to date to unravel the mechanisms underlying AQM [23, 37, 38]. These experiments have resulted in a number of interesting observations, but our results lead us to question whether the loss of an intact motoneuron and continued mechanical loading in freely moving rats is a suitable model for the muscle wasting in ICU patients in general and AQM patients in particular. Although a detailed histopathological evaluation of the muscle samples is beyond the scope of this study, it is interesting to note that the regional loss or uneven mATPase staining observed in the soleus muscle in response to NMB resembles the histopathological changes reported in AQM patients (Fig. 1; [29]). Three weeks of peripheral denervation, on the other hand, had no significant effect on mATPase staining.

Effects of NMB on different muscles and muscle types

In contrast to the muscle-type-specific effects of denervation on myosin–actin protein and mRNA ratios, fast- and slow-twitch muscles (EDL and soleus, respectively) responded in a similar way to the muscle wasting model used in this study. The parallel changes at the protein and mRNA levels, although not statistically significant, i.e., trend at the mRNA level, support a transcriptional regulation of myofibrillar protein synthesis, which contrasts with the dissociation of myosin–actin protein and mRNA ratios by denervation in the slow-twitch soleus.

Respiratory muscles differ in their physiological demands compared with postural and locomotor muscles; the continuous motor activity during respiration makes them among the most active skeletal muscles in the body [40]. The effects of mechanical ventilation on diaphragm structure, function and myofibrillar protein and mRNA expression have received significant attention in the past decade, but information on the intercostal muscles is sparse. The mechanical ventilation effects on the diaphragm have typically been studied for 24 h or less [34, 36, 41, 43, 44, 53], but mechanical ventilation for ≤4 days have been published in two independent studies [41, 51], as well as the effects of 5 days of mechanical ventilation on the diaphragm in a porcine model [12, 35, 36]. However, critically ill ICU patients are often mechanically ventilated for significantly longer time periods, i.e., weeks–months. The short-term effects of mechanical ventilation and muscle activity have collectively shown a decrease in diaphragm force, increased proteolytic activity and decreased overall protein synthesis rate during the first 12 h of mechanical ventilation. During this initial phase, the decreased protein synthesis rate was primarily related to translational events and no changes were observed in MyHC mRNA expression [45]. Thus, during the early phase of mechanical ventilation, protein degradation and decreased protein synthesis at the post-transcriptional level appear to play a dominating role. However, it has been suggested that transcription may play an important role in regulating myofibrillar protein synthesis in response to longer periods of inactivity, i.e., days–weeks [45]. This is consistent with the present observations in the hind limb and intercostal muscles.

While the diaphragm and intercostal muscles are among the most active skeletal muscles in the body, there are significant differences between the two muscles. The intercostal muscles have both respiratory and postural motor functions and have origin and insertion attach to bone, leading to activation and loading conditions that are different from those of the diaphragm (see [40]). For the intercostals, the changes in MyHC mRNA and myosin–actin protein and mRNA expression were very similar to the pattern observed in the fast- and slow-twitch hind limb muscles, i.e., a dramatic down-regulation of myosin mRNA levels and decreased myosin–actin ratios at the protein and mRNA levels. For the diaphragm, only a small decrease was conversely observed in total myosin mRNA levels, there were no signs of a preferential myosin loss at the protein level, and the myosin–actin mRNA ratio increased in contrast to the decreased mRNA ratio in limb and intercostal muscles. These results collectively indicate a transcriptional regulation of myofibrillar protein synthesis in the intercostal muscles, but not in the diaphragm. The diaphragm is a unique muscle and the exact mechanism underlying the different response to post-synaptic neuro-

muscular blockade, unloading and mechanical ventilation compared with intercostals remains unknown.

As discussed above, the mechanical loading of the sarcomere is expected to have a significant impact on transcriptional regulation of myofibrillar protein synthesis and degradation, e.g., via the titin kinase [27]. In the absence of excitation–contraction coupling due to NMB, the mechanical loading of the sarcomere caused by myosin–actin interactions during contraction was eliminated in all investigated muscles. However, the passive loading of the respiratory muscles induced by the mechanical ventilator was not sufficient to eliminate the transcriptional down-regulation of myofibrillar proteins in the intercostal muscles. It cannot be excluded that the dissimilarity in myofibrillar protein and mRNA expression between the two respiratory muscles in NMB rats is related to the differences in sensitivity to mechanical load. However, experiments using unilateral inactivation of the diaphragm by denervation or tetrodotoxin treatment suggest that mechanical loading is not the primary determinant of structural adaptations of the diaphragm muscle, i.e., compensatory changes in muscle fibre size were not related to loading [40]. The phrenic nerve trophic influence on the diaphragm has been forwarded as a key factor in maintaining diaphragm structure and function. Further studies are needed to explore the potential role for neurotrophic factors specifically influencing the diaphragm muscle [40].

The cranial-nerve-innervated masseter muscle responded differently to NMB, unloading and ventilation than the spinal-nerve-innervated limb and intercostal muscles. In the NMB rats, the masseter was affected less, if at all, than the limb and intercostal muscles. This result accords with clinical data on the muscle wasting and paralysis in ICU patients with AQM [6, 14, 18, 29]. No significant differences were observed in the mRNA expression for specific isoforms, total mRNA or myosin–actin mRNA ratios for the masseter, although a small decline in the myosin–actin protein ratio was observed.

The concept of allotype was introduced by Hoh and Hughes [22] to identify fundamentally distinct skeletal muscle classes, each of which have a specific intrinsic range of phenotypic options for myosin gene expression in mature myofibres [21]. The identified skeletal muscle allotypes include limb, diaphragm, masticatory and extraocular muscles, and it has been suggested that laryngeal and middle ear muscle may also prove to be distinct allotypes [33]. The differences between muscle fibres in the reaction to interventions cannot be predicted based upon muscle phenotype [21]. Thus, the observed differences in MyHC expression responsiveness to NMB, unloading and ventilation appear to be allotype specific, suggesting that the intercostal muscles belong to the same allotype as the limb muscles. The responsiveness of one muscle allotype to an intervention, such as NMB, cannot be generalised to all skeletal muscles. Therefore, the inclusion of muscles representing different allotypes is essential in understanding the muscle wasting in ICU patients.

Effects of NMB on MyBP-C and MyBP-H mRNA expression

Next to myosin, the myosin-binding proteins MyBP-C and -H are the most abundant proteins in the thick filament, representing up to 4% of myofibril mass [47], and both MyBP-C and MyBP-H play an important role during myofibrillogenesis by binding to myosin and regulating the organisation of the motor protein within the thick filament (see [42]). Furthermore, MyBP-C has been suggested to play a physiological role by modulating contraction via an influence on cross-bridge motion effects on the S-2 region of myosin or by cross-linking myosin and actin (e.g., [19, 20]). In human limb muscles, a coordinated expression of MyHC and MyBP-C isoforms are observed at the single muscle fibre, but this coordination is not observed in the masseter [52].

A down-regulation of MyBP-C was observed in the EDL and the soleus from NMB and DEN rats, but not in the two respiratory muscles or in the masseter. The MyBP-H mRNA levels, on the other hand, were increased in all muscles in response to NMB, unloading and ventilation. MyBP-C and MyBP-H share considerable sequence homology over their C-termini, but they differ significantly at the N-termini. The variability within the N-terminal regions may play a significant role in defining additional protein–protein interactions, in final placement in the sarcomere and in protein function [1]. Thus, the transcriptional regulation of the myosin-associated proteins does not follow the same muscle allotype pattern as for myosin in the NMB animals. Furthermore, MyBP-H mRNA expression was completely different from MyBP-C, supporting a different role of these proteins in the sarcomere, and it is hypothesised that the up-regulation of MyBP-H may represent an early sign of muscle regeneration.

Conclusion

The mechanisms of the muscle wasting in ICU patients exposed to pharmacological neuromuscular block, muscle unloading and mechanical ventilation are critical to explaining and alleviating the prolonged impaired quality of life that many of these patients experience. In the rat ICU model used in this study, the animals were exposed to a very similar pharmacological neuromuscular block, muscle unloading and mechanical ventilation for 7–13 days.

Decreased body weight, muscle mass, muscle fibre atrophy, decreased protein synthesis and altered myosin–actin ratios were observed in all animals. However, the responsiveness of myofibrillar protein and mRNA expression to these interventions varied between muscles (allotypes). In addition, significant muscle-specific differences were observed in the transcriptional regulation between myosin, myosin-binding proteins and actin, indicating that factors other than muscle allotype may influence the responsiveness of muscle to ICU-like conditions.

The animal model used in this study is advanced as a suitable experimental animal model for studying the effects of ICU care on skeletal muscle. Not only does this model possess characteristics of the disease, i.e., decrease in muscle mass, decreased myosin–actin ratio, decrease in myosin mRNA and masticatory muscles being less affected than limb muscles, but it may also provide insight into the acute stages of the disease and the relative importance of potential causative agents.

Acknowledgements We are grateful to Susan Dworkin, Yvette Hedström and Helena Svahn for excellent technical assistance. This study was supported by grants from NIH (HL040837 and AR045627) to BRD and (AR 045627, AR 047318 and AG014731), the Swedish Cancer Society and the Swedish Research Council (08651) to L.L.

References

1. Alyonycheva TN, Mikawa T, Reinach FC, Fischman DA (1997) Isoform-specific interaction of the myosin-binding proteins (MyBPs) with skeletal and cardiac myosin is a property of the C-terminal immunoglobulin domain. J Biol Chem 272:20866–20872
2. Ansved T, Larsson L (1990) Effects of denervation on enzyme—histochemical and morphometrical properties of the rat soleus muscle in relation to age. Acta Physiol Scand 139:297–304
3. Booth FW (1982) Effect of limb immobilization on skeletal muscle. J Appl Physiol 52:1113–1118
4. Booth FW, Kirby CR (1992) Changes in skeletal muscle gene expression consequent to altered weight bearing. Am J Physiol 262:R329–R332
5. Boudriau S, Cote CH, Vincent M, Houle P, Tremblay RR, Rogers PA (1996) Remodeling of the cytoskeletal lattice in denervated skeletal muscle. Muscle Nerve 19:1383–1390
6. Danon MJ, Carpenter S (1991) Myopathy with thick filament (myosin) loss following prolonged paralysis with vecuronium during steroid treatment. Muscle Nerve 14:1131–1139
7. De Letter MA, van Doorn PA, Savelkoul HF, Laman JD, Schmitz PI, Op de Coul AA, Visser LH, Kros JM, Teepen JL, van der Meche FG (2000) Critical illness polyneuropathy and myopathy (CIPNM): evidence for local immune activation by cytokine-expression in the muscle tissue. J Neuroimmunol 106206–213
8. Di Giovanni S, Molon A, Broccolini A, Melcon G, Mirabella M, Hoffman EP, Servidei S (2004) Constitutive activation of MAPK cascade in acute quadriplegic myopathy. Ann Neurol 55:195–206
9. Dworkin BR, Dworkin S (1991) Verification of skeletal activity in tibial nerve recordings: a reply to Roberts (1991). Behav Neurosci 105:773–779
10. Dworkin BR, Dworkin S, Tang X (2000) Carotid and aortic baroreflexes of the rat: I. Open-loop steady-state properties and blood pressure variability. Am J Physiol Regul Integr Comp Physiol 279:R1910–R1921
11. Fitts RH, Metzger JM, Riley DA, Unsworth BR (1986) Models of disuse: a comparison of hindlimb suspension and immobilization. J Appl Physiol 60:1946–1953
12. Fredriksson K, Radell P, Eriksson LI, Hultenby K, Rooyackers O (2005) Effect of prolonged mechanical ventilation on diaphragm muscle mitochondria in piglets. Acta Anaesthesiol Scand 49:1101–1107
13. Giulian GG, Moss RL, Greaser M (1983) Improved methodology for analysis and quantitation of proteins on one-dimensional silver-stained slab gels. Anal Biochem 129:277–287
14. Gooch JL, Suchyta MR, Balbierz JM, Petajan JH, Clemmer TP (1991) Prolonged paralysis after treatment with neuromuscular junction blocking agents. Crit Care Med 19:1125–1131
15. Haddad F, Herrick RE, Adams GR, Baldwin KM (1993) Myosin heavy chain expression in rodent skeletal muscle: effects of exposure to zero gravity. J Appl Physiol 75:2471–2477
16. Helliwell TR, Wilkinson A, Griffiths RD, McClelland P, Palmer TE, Bone JM (1998) Muscle fibre atrophy in critically ill patients is associated with the loss of myosin filaments and the presence of lysosomal enzymes and ubiquitin. Neuropathol Appl Neurobiol 24:507–517
17. Herridge MS, Cheung AM, Tansey CM, Matte-Martyn A, Diaz-Granados N, Al-Saidi F, Cooper AB, Guest CB, Mazer CD, Mehta S, Stewart TE, Barr A, Cook D, Slutsky AS (2003) One-year outcomes in survivors of the acute respiratory distress syndrome. N Engl J Med 348:683–693
18. Hirano M, Ott BR, Raps EC, Minetti C, Lennihan L, Libbey NP, Bonilla E, Hays AP (1992) Acute quadriplegic myopathy: a complication of treatment with steroids, nondepolarizing blocking agents, or both. Neurology 42:2082–2087
19. Hofmann PA, Greaser ML, Moss RL (1991) C-protein limits shortening velocity of rabbit skeletal muscle fibres at low levels of Ca^{2+} activation. J Physiol 439:701–715
20. Hofmann PA, Hartzell HC, Moss RL (1991) Alterations in Ca^{2+} sensitive tension due to partial extraction of C-protein from rat skinned cardiac myocytes and rabbit skeletal muscle fibers. J Gen Physiol 97:1141–1163
21. Hoh JF (1991) Myogenic regulation of mammalian skeletal muscle fibres. News Physiol Sci 6:1–6
22. Hoh JF, Hughes S (1989) Immunocytochemical analysis of the perinatal development of cat masseter muscle using anti-myosin antibodies. J Muscle Res Cell Motil 10:312–325
23. Horinouchi H, Kumamoto T, Kimura N, Ueyama H, Tsuda T (2005) Myosin loss in denervated rat soleus muscle after dexamethasone treatment. Pathobiology 72:108–116
24. Hudson LD, Lee CM (2003) Neuromuscular sequelae of critical illness. N Engl J Med 348:745–747
25. Jakubiec-Puka A (1992) Changes in myosin and actin filaments in fast skeletal muscle after denervation and self-reinnervation. Comp Biochem Physiol Comp Physiol 102:93–98
26. Lange S, Ehler E, Gautel M (2005) From A to Z and back? Multicompartment proteins in the sarcomere. Trends Cell Biol 16 (1):11–18
27. Lange S, Xiang F, Yakovenko A, Vihola A, Hackman P, Rostkova E, Kristensen J, Brandmeier B, Franzen G, Hedberg B, Gunnarsson LG, Hughes SM, Marchand S, Sejersen T, Richard I, Edstrom L, Ehler E, Udd B, Gautel M (2005) The kinase domain of titin controls muscle gene expression and protein turnover. Science 308:1599–1603
28. Larsson L, Edstrom L, Lindegren B, Gorza L, Schiaffino S (1991) MHC composition and enzyme-histochemical and physiological properties of a novel fast-twitch motor unit type. Am J Physiol 261:C93–C101

29. Larsson L, Li X, Edstrom L, Eriksson LI, Zackrisson H, Argentini C, Schiaffino S (2000) Acute quadriplegia and loss of muscle myosin in patients treated with nondepolarizing neuromuscular blocking agents and corticosteroids: mechanisms at the cellular and molecular levels. Crit Care Med 28:34–45
30. Larsson L, Moss RL (1993) Maximum velocity of shortening in relation to myosin isoform composition in single fibres from human skeletal muscles. J Physiol 472:595–614
31. Loughna PT, Morgan MJ (1999) Passive stretch modulates denervation induced alterations in skeletal muscle myosin heavy chain mRNA levels. Pflugers Arch 439:52–55
32. Metafora S, Felsani A, Cotrufo R, Tajana GF, Di Iorio G, Del Rio A, De Prisco PP, Esposito V (1980) Neural control of gene expression in the skeletal muscle fibre: the nature of the lesion in the muscular protein-synthesizing machinery following denervation. Proc R Soc Lond B Biol Sci 209: 239–255
33. Porter JD, Baker RS (1996) Muscles of a different 'color': the unusual properties of the extraocular muscles may predispose or protect them in neurogenic and myogenic disease. Neurology 46:30–37
34. Powers SK, Shanely RA, Coombes JS, Koesterer TJ, McKenzie M, Van Gammeren D, Cicale M, Dodd SL (2002) Mechanical ventilation results in progressive contractile dysfunction in the diaphragm. J Appl Physiol 92:1851–1858
35. Radell P, Edstrom L, Stibler H, Eriksson LI, Ansved T (2004) Changes in diaphragm structure following prolonged mechanical ventilation in piglets. Acta Anaesthesiol Scand 48:430–437
36. Radell PJ, Remahl S, Nichols DG, Eriksson LI (2002) Effects of prolonged mechanical ventilation and inactivity on piglet diaphragm function. Intensive Care Med 28:358–364
37. Rich MM, Kraner SD, Barchi RL (1999) Altered gene expression in steroid-treated denervated muscle. Neurobiol Dis 6:515–522
38. Rich MM, Pinter MJ, Kraner SD, Barchi RL (1998) Loss of electrical excitability in an animal model of acute quadriplegic myopathy. Ann Neurol 43:171–179
39. Rouleau G, Karpati G, Carpenter S, Soza M, Prescott S, Holland P (1987) Glucocorticoid excess induces preferential depletion of myosin in denervated skeletal muscle fibers. Muscle Nerve 10:428–438
40. Rowley KL, Mantilla CB, Sieck GC (2005) Respiratory muscle plasticity. Respir Physiol Neurobiol 147:235–251
41. Sassoon CS, Caiozzo VJ, Manka A, Sieck GC (2002) Altered diaphragm contractile properties with controlled mechanical ventilation. J Appl Physiol 92:2585–2595
42. Seiler SH, Fischman DA, Leinwand LA (1996) Modulation of myosin filament organization by C-protein family members. Mol Biol Cell 7:113–127
43. Shanely RA, Coombes JS, Zergeroglu AM, Webb AI, Powers SK (2003) Short-duration mechanical ventilation enhances diaphragmatic fatigue resistance but impairs force production. Chest 123:195–201
44. Shanely RA, Zergeroglu MA, Lennon SL, Sugiura T, Yimlamai T, Enns D, Belcastro A, Powers SK (2002) Mechanical ventilation-induced diaphragmatic atrophy is associated with oxidative injury and increased proteolytic activity. Am J Respir Crit Care Med 166:1369–1374
45. Shanley CJ, Bartlett RH (1994) The management of acute respiratory failure. Curr Opin Gen Surg:7–16
46. Showalter CJ, Engel AG (1997) Acute quadriplegic myopathy: analysis of myosin isoforms and evidence for calpain-mediated proteolysis. Muscle Nerve 20:316–322
47. Starr R, Offer G (1971) Polypeptide chains of intermediate molecular weight in myosin preparations. FEBS Lett 15:40–44
48. Stevenson EJ, Giresi PG, Koncarevic A, Kandarian SC (2003) Global analysis of gene expression patterns during disuse atrophy in rat skeletal muscle. J Physiol 551:33–48
49. Tajsharghi H, Thornell LE, Darin N, Martinsson T, Kyllerman M, Wahlstrom J, Oldfors A (2002) Myosin heavy chain IIa gene mutation E706K is pathogenic and its expression increases with age. Neurology 58:780–786
50. Talmadge RJ, Roy RR, Bodine-Fowler SC, Pierotti DJ, Edgerton VR (1995) Adaptations in myosin heavy chain profile in chronically unloaded muscles. Basic Appl Myol 5:117–137
51. Yang L, Luo J, Bourdon J, Lin MC, Gottfried SB, Petrof BJ (2002) Controlled mechanical ventilation leads to remodeling of the rat diaphragm. Am J Respir Crit Care Med 166:1135–1140
52. Yu F, Stal P, Thornell LE, Larsson L (2002) Human single masseter muscle fibers contain unique combinations of myosin and myosin binding protein C isoforms. J Muscle Res Cell Motil 23:317–326
53. Zhu E, Sassoon CS, Nelson R, Pham HT, Zhu L, Baker MJ, Caiozzo VJ (2005) Early effects of mechanical ventilation on isotonic contractile properties and MAF-box gene expression in the diaphragm. J Appl Physiol 99:747–756